Competition between slicing and buckling underlies the erratic nature of paper cuts

Sif Fink Arnbjerg-Nielsen, Matthew D. Biviano, and Kaare H. Jensen*
Department of Physics, Technical University of Denmark, DK-2800 Kongens Lyngby, Denmark

(Received 31 January 2024; revised 24 May 2024; accepted 19 June 2024; published 23 August 2024)

By enabling the dissemination and storage of information, paper has been central to human culture for more than a millennium. Its use is, however, associated with a common injury: the paper cut. Surprisingly, the physics underpinning a flexible sheet of paper slicing into soft tissues remains unresolved. In particular, the unpredictable occurrence of paper cuts, often restricted to a limited thickness range, has not been explained. Here we visualize and quantify the motion, deformation, and stresses during paper cuts, uncovering a remarkably complex relationship between cutting, geometry, and material properties. A model based on the hypothesis that a competition between slicing and buckling controls the probability of initiating a paper cut is developed and successfully validated. This explains why paper with a specific thickness is most hazardous (65 μm, corresponding, e.g., to dot matrix paper) and suggests a probabilistic interpretation of irregular occurrence of paper cuts. Stimulated by these findings, we finally show how a recyclable cutting tool can harness the surprising power of paper.

DOI: 10.1103/PhysRevE.110.025003

I. INTRODUCTION

Paper cuts are a common injury that can cause significant pain and discomfort [1]. It is endemic among literate persons (globally 86% aged 15+ years [2]) and may lead to severe microbial infections [3,4]. Despite its widespread occurrence, however, the physical mechanism that allows certain types of paper to cut into the skin, but precludes others, remains poorly understood [5].

A particular mystery surrounds the link between paper thickness and the occurrence of cuts, often described as unpredictable and erratic. Fine, thin, and sharp blades have long been preferred, "for bluntness is a cause of great pain" (Julius Africanus, c. 200 CE [6]), and are currently in widespread use [7]. However, this principle does not hold for paper cuts. Injuries often occur while handling a magazine or office paper (thickness $t \approx 0.05 - 0.10$ mm). In contrast, tissues ($t \approx 0.03$ mm), as well as postcards ($t \approx 0.2$ mm), are generally considered safe (Fig. 1). The restricted occurrence of paper cuts in a limited thickness range has not been explained [5].

In this letter, we combine experiments and theory to map the mechanics of paper cutting into a soft solid. Two parameters are explored: the paper thickness t and the slicing angle ϕ, which is a key parameter for rigid blades [8–10], wire cutters [11,12], and paper cuts [13]. Our experiments reveal that for paper blades, a competition between slicing and buckling controls the cutting process. This provides a simple framework for understanding the erratic nature of paper cuts and lays the foundation for physics-informed design of paper-based blades.

II. METHODS

To quantify if and when paper can cut a soft solid, we attempted to slice into a piece of freshly prepared gelatin using a variety of paper sheets (Table I, Fig. 1). The paper specimens were chosen for broad coverage and availability (see Appendix E, Table I [14]). The standardized paper sample was a rectangle of length $\ell = 10$ cm and thickness $t = 0.025$–0.25 mm sandwiched between two 3D-printed elements parallel to the paper edge [Fig. 2(a)]. When handling paper, for instance, when turning the page of a journal, a book, or a newspaper, we often fix the sheet using one finger while trying to peel or lift the edge using another finger. The characteristic paper height (h) can thus be objectively defined as the typical thickness of a finger. The value used here ($h = 14$ mm) corresponds to the size of an index finger of Western children and adults [15]. The elastic modulus $E_s \approx 3$ kPa of the gelatin (Bloom 230, 10% wt, dissolved in water at 75°–100°C and set for 26–29 h at 20°) was measured using a rectangular punch indentation test [16] (see Fig. 6). The gelatin sample was a slab of length $L = 7$ mm, thickness $T = 40$ mm, and height $H = 10$ mm, fixed at the bottom and on the two sides parallel to the paper blade. The sample dimensions and properties were again chosen based on human limb sizes [17,18]. The cutting edge remained parallel to the cutting surface along the y-axis throughout the experiments [Fig. 2(a)]. The cutting speed (typically 2.8 mm/s) was controlled by mounting the paper clamp on a two-axis stage driven by servomotors (MPC-200/MP-285, Sutter Instruments, USA). We varied the cutting angle ϕ by modifying the y- and z-velocity components to explore the role of shear in the cutting process from $\phi = 5°$ (motion almost parallel to the surface) to $\phi = 90°$ (normal motion). The vertical indentation depth $d = 2$ mm of the paper sheet post contact with the gelatin block was kept constant. The deformation and cutting processes were recorded with a video camera (camera: acA1920-uc, Basler AG, Germany, lens: AF-P DX Nikkor 18-55mm f/3.5-5.6G VR, Nikon, Japan). Normal (σ_n) and shear (σ_t) stresses induced by the slicing motion ($\tan\phi = \sigma_n/\sigma_t$) were measured using two orthogonally mounted force sensors (TAL221 100g load cell, SparkFun Electronics, USA, amplifier: Mini Weight

*Contact author: khjensen@dtu.dk

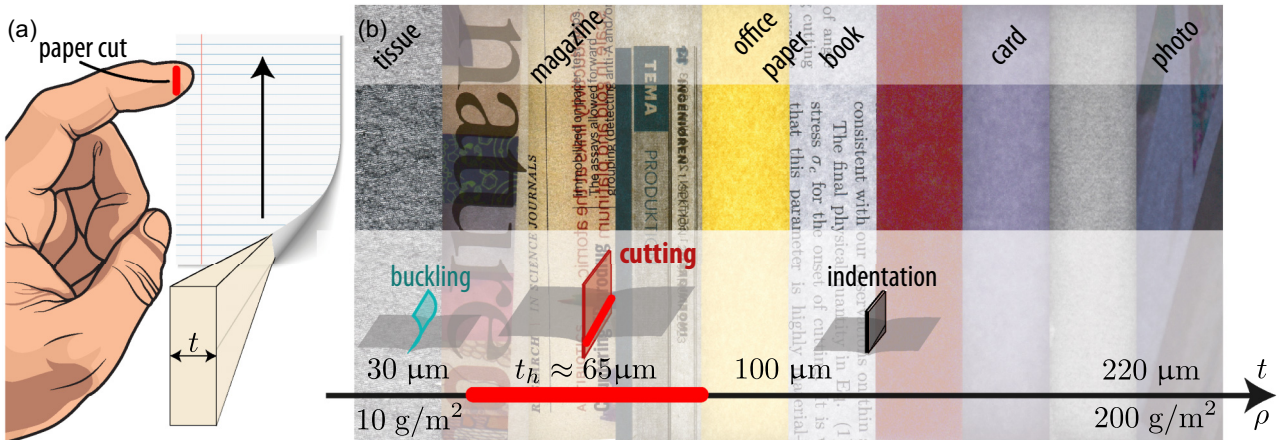

FIG. 1. The physics of paper cuts. (a) Paper cuts are a common injury that can occur if skin contacts a sheet of paper (thickness t, area density ρ). It causes significant pain and discomfort and is often associated with a slicing motion (arrow). The underlying physical processes remain poorly understood. (b) However, it is well established that cuts frequently occur in the thickness range of $t = 0.05$-0.1 mm (this range includes magazines and office paper) [5], whereas thinner and thicker paper is relatively safe. We propose that a competition between slicing and buckling determines which paper types can cut. If the sheet is too thin, it buckles and loses structural integrity before initiating a fracture. In contrast, thicker sheets smoothly indent the surface and distribute the load over a greater area. The slicing motion enhances the likelihood of cutting, which peaks at the most hazardous thickness $t_h \approx 65$ μm (see Fig. 2).

Unit HX711, M5Stack, China). Young's modulus of paper was measured by a cantilever bending test [19]. See the Supplemental Material (Data S1) for CAD drawings [14].

III. RESULTS

A. Experiments

Each paper sample's cutting dynamics are unique, but clear patterns allow us to divide the data into three rough categories (Figs. 2 and 5, and Supplemental Video S1 [14]). To unpack the relevant physical processes, we begin by considering the performance of a relatively thick sheet ($t = 0.22$ mm) at a fixed slicing angle, say $\phi \approx 15°$ [Fig. 2(d)]. In this case, the normal stress σ_n increases rapidly as the paper pushes against the gelatin until reaching peak applied stress, σ_a, whereas the tangential load σ_t grows but remains comparatively small. Although the gelatin is strongly deformed in the vertical direction (Supplemental Video S1 [14]), the paper retains its shape, and a visual inspection of the substrate surface before and after the experiment reveals that no cutting has occurred (Fig. 5). Apparently, the applied stress σ_a remained below the critical value $\sigma_{n,c}$ required to initiate cutting (see, e.g., Refs. [8,11,20]).

For a moderately thin sheet ($t = 0.105$ mm) in the same slicing conditions ($\phi = 15°$), however, the situation is completely different [Fig. 2(c)]. Here, the tangential load increases superlinearly after the cut is initiated. The sheet remains rigid during the experiment but cleanly cuts into

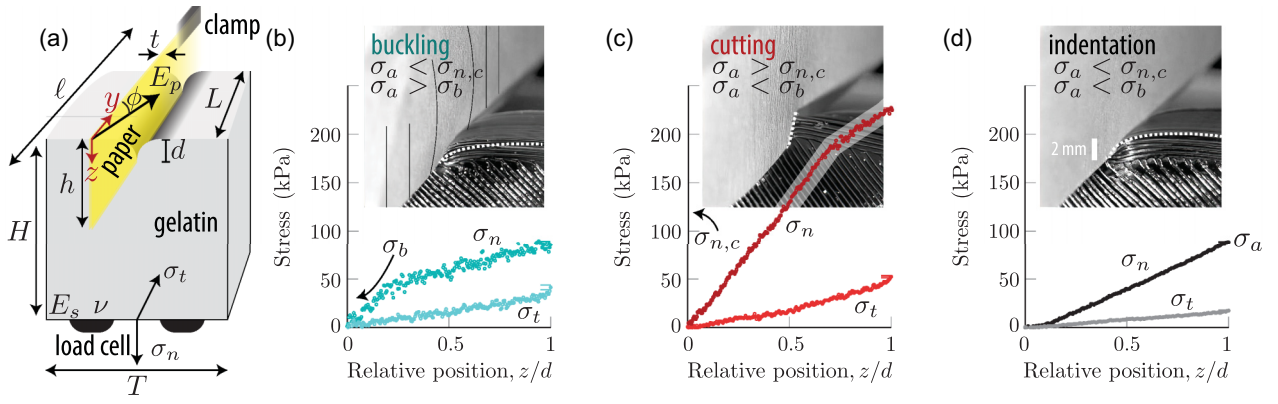

FIG. 2. Experimental setup and data classification scheme. (a) Schematic of the experiment used to quantify contact processes between a soft solid and a sheet of paper in relative motion. The standardized paper and gelatin samples were held by 3D-printed clamps. The vertical indentation depth, d, the speed (arrow), and the slicing angle ϕ of the paper sheet were controlled using a micromanipulator. A video of each experiment was recorded and the stresses [normal (σ_n) and tangential (σ_t) to the gelatin surface] were measured using two load cells. (b–d) Representative data illustrating three regimes. (b) Thin paper ($t = 30$ μm, $\phi = 15°$) buckles because the normal load exceeds the buckling threshold σ_b before reaching peak applied stress, $\sigma_a > \sigma_b$. (c) Intermediate paper ($t = 65$ μm, $\phi = 15°$) cuts because the cutting threshold $\sigma_{n,c}$ is exceeded before reaching σ_b or σ_a. (d) Finally, thick paper ($t = 220$ μm, $\phi = 15°$) indents the surface because the dispersed normal force is insufficient to breach the surface or buckle the paper. (See also Supplemental Video S1 [14] and additional details in the text.)

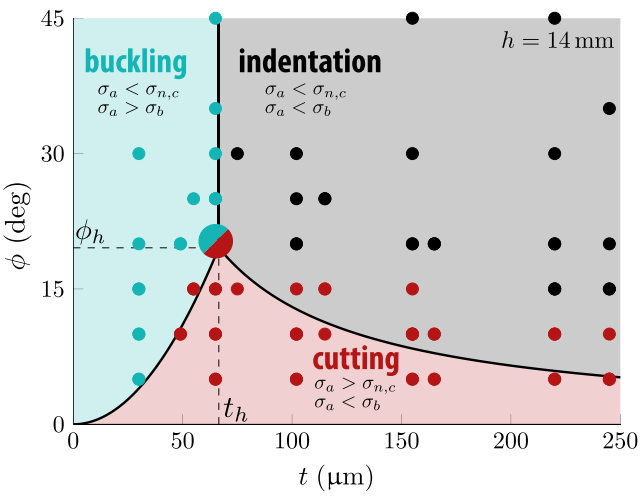

FIG. 3. A competition between slicing and buckling governs paper cuts. The phase diagram shows the outcome of each experiment (dots) as a function of thickness t and slicing angle ϕ. The outcome of a cutting attempt depends on how the thresholds relate to each other. If $\phi < \phi_h$, then there exists a range of thicknesses for which $\sigma_{n,c}$ is lower than both σ_a and σ_b where cutting is observed. When the slicing angle ϕ is sufficiently small, nearly all types of paper cuts (red shaded domain, label: cutting). However, the probability peaks at the most hazardous thickness $t_h \approx 65\,\mu\mathrm{m}$ (between printed magazines and office paper) and angle $\phi_h \approx 20^\circ$. Outside this zone, the peak applied stress either exceeds the buckling limit (label: buckling) or simply causes an indentation (label: indentation) (top right). The mechanical model [Eqs. (1)–(4)] is consistent with observations (solid lines mark model transitions between domains). Error bars: $t \pm 5\,\mu\mathrm{m}$ and $\phi \pm 2^\circ$. See additional details in the text.

the sample, leaving a permanent scar on the gelatin surface. Because the comparatively thinner sheet applied nearly the same peak force to the slab, the peak applied stress σ_a (force per contact area), exceeding the critical level $\sigma_{n,c}$ required to initiate cutting in this case.

The final data category captures the behavior of relatively thin sheets (e.g., $t = 0.03$ mm, $\phi = 15^\circ$). Here, the tangential force again increases linearly, whereas the normal load trajectory has a distinct kink [Fig. 2(b)]: shortly following contact, the thin sheet is bent out of shape by the applied load. It then slides along the slab, sometimes leaving minor residual abrasion damage on the surface. Presumably, the unsuccessful cutting results from the paper buckling at the stress σ_b below the critical cutting value $\sigma_{n,c}$.

Having established the three basic data categories (indentation, cutting, and buckling), we will now examine the influence of the slicing angle ϕ. To facilitate this discussion, we position our data in a phase diagram as a function of the sheet thickness t and the cutting angle ϕ (Fig. 3). The aforementioned transition from indentation to cutting and buckling with diminishing paper thickness is consistently observed for angles in the range $\phi = 10^\circ - 25^\circ$. We did not detect cutting for angles $\phi > 25^\circ$. Additionally, the data suggest that the range of paper thicknesses able to cut broadens dramatically when the slicing angle diminishes. However, the physical reason for the data tripartition remains unknown.

B. Physical model

To rationalize the experimental data, we develop a simple mathematical model of paper cutting into a soft material. The process can be studied in full detail using direct numerical simulations, for example, with finite element methods [8,11,12]. However, here we focus on the fundamental physical phenomena and attempt to derive scaling relations to explain the phase diagram's critical features (Fig. 3).

We begin by stating the basic fact that for successful cutting, the normal stress σ_n must, at some point during the cutting attempt, exceed the critical threshold $\sigma_{n,c}$ required to cut. However, it should not grow larger than the buckling limit σ_b at which the paper loses most ability to convert the vertical strain into stress. Recall that during the slicing process, σ_n increases from zero (initial contact) to its peak value σ_a when the paper has moved a distance d along the vertical axis [Fig. 2(d)]. The peak applied stress must therefore obey the inequality

$$\sigma_{n,c} < \sigma_a < \sigma_b, \tag{1}$$

which, as shown below, explains the three distinct regions in the phase diagram (Fig. 3).

To unpack the physical meaning of the cutting inequality [Eq. (1)], we begin by considering the magnitude of the peak applied stress, σ_a. The interaction between the paper sheet and the gelatin sample can be approximated as a uniform indentation of a rigid rectangular punch into an elastic half-space [16], in which case the average peak applied stress is

$$\sigma_a = \frac{\pi}{2\ln 2}\frac{E_s}{1-\nu^2}\frac{d}{t}, \tag{2}$$

where $\nu \approx 0.5$ is Poisson's ratio [Fig. 2(a)]. As expected, the peak applied stress $\sigma_a \sim t^{-1}$ scales inversely with the paper thickness t and linearly with the indentation depth d (c.f. Hooke's law). Similarly, the buckling threshold stress σ_b can be found from beam theory [21]

$$\sigma_b = \kappa E_p \frac{t^2}{h^2}, \tag{3}$$

where $E_p \approx 7.5$ GPa is the elastic modulus of paper in the thin range of the tested range (Appendix E, Table I), t is the thickness, and h is the height of the paper blade [Fig. 1(a)]. The prefactor $\kappa = \pi^2/(12K^2)$ is determined by the boundary conditions for the buckling blade. In our case, one end is pinned while the other is fixed, corresponding to $K \approx 0.70$ such that $\kappa \approx 1.68$. The scaling $\sigma_b \sim t^2$ is consistent with our observations on thin sheets (Fig. 7). It is possible to consider plate-like flexural instabilities using detailed numerical simulations (e.g., Ref. [22]), but we will not do that here.

The final physical quantity in the inequality (1) is the normal stress $\sigma_{n,c}$ at the onset of cutting. Soft solids can typically resist large compressive stresses but fail under a critical tensile stress $\sigma_{t,c}$ that might result from a combination of compression and/or shear. For gelatin and human skin, cutting stresses are of the order 0.1–1 MPa [23,24]. It is well established that the tensile stress required to initiate cutting depends on the fracture toughness and Young's modulus, and that it can be affected by, for example, aging and environmental factors

such as temperature and humidity [11,12,23,25–27]. Surface abrasion caused by dynamic (sliding) friction may also lower the cutting stress. However, the residual abrasion damage did not exceed the imperfections caused by the fabrication process. Evidence thus does not suggest that friction in the parallel motion played a critical role in the onset of cutting.

For combined normal and tangential loading, the largest tensile stress equals the shear stress σ_t [11]. An essential feature of slicing soft materials is therefore that the normal stress $\sigma_{n,c}$ necessary for cutting [c.f. Eq. (1)] varies with the slicing angle ϕ because of the direct coupling to the shear component (recall $\sigma_n = \sigma_t \tan\phi$). We can therefore approximate the critical normal stress by a linear angular dependence

$$\sigma_{n,c} \approx \sigma_{t,c}\,\phi. \tag{4}$$

Experimentally, the linear relation is consistent with experimental data beyond the validity of the small angle approximation ($\sigma_{t,c} = 0.84$ MPa, see Fig. 8). At $\phi \approx 30^\circ$, the Taylor expansion deviates with 10%. We note that cutting phenomena at $\phi = 0^\circ$ are not described by this model.

When taken together, Eqs. (1)–(4) reveal a basic physical explanation of the phase diagram domains: only certain combinations of paper thickness and slicing angle can generate enough stress to cut into the substrate. Specifically, for a fixed slicing angle ϕ, the cutting threshold normal stress $\sigma_{n,c}(\phi)$ is a constant [Eq. (4)]. However, the peak applied stress $\sigma_a \sim t^{-1}$ increases when the paper thickness t diminishes, whereas the paper becomes more prone to buckling. The outcome thus depends on which of the two thresholds will be reached first: cutting $\sigma_{n,c}$ [Eq. (4)] or buckling $\sigma_b \propto t^2$ [Eq. (3)]. The most hazardous paper thickness t_h (for which cutting is possible for the greatest range of angles) corresponds to the case where the peak applied stress, buckling threshold, and cutting threshold are equal (i.e., $\sigma_a = \sigma_b = \sigma_{n,c}$). Equating Eqs. (2) and (3) leads to an expression for the most hazardous paper thickness in terms of the system parameters

$$t_h = \alpha\left(\tfrac{1}{1-\nu^2}\tfrac{E_s}{E_p}h^2 d\right)^{1/3} \approx 65\,\mu\text{m}, \tag{5}$$

where $\alpha = [\pi/(2\kappa \ln 2)]^{1/3} \approx 1.1$ is a numerical constant.

The largest angle at which cutting is observed for a given thickness t—that is, the line delimiting the cutting regime from the other domains in the phase diagram (Fig. 3) is given by

$$\phi_c(t) = \begin{cases} \kappa \frac{E_p}{\sigma_{t,c}} \frac{t^2}{h^2} & \text{if } t \leqslant t_h \\ \frac{\pi}{2\ln 2(1-\nu^2)} \frac{E_s}{\sigma_{t,c}} \frac{d}{t} & \text{if } t \geqslant t_h \end{cases}. \tag{6}$$

From this follows $\phi_h = \phi_c(t_h) \approx 19^\circ$ (i.e., no paper will cut at angles larger than 19°).

Notably, the most hazardous thickness t_h scales relatively weakly (i.e., to the $1/3$ power) with the material and geometric parameters. In most realistic cases, it therefore deviates relatively little from the estimate $t_h \approx 65\,\mu$m, near, for instance, magazines and dot matrix paper (Appendix E, Table I [14]). It should be noted that the free height h influences the transitions between domains in the phase diagram. A phase diagram for $h = 28$ mm is not inconsistent with the prediction that t_h increases and ϕ_h decreases with h (see Fig. 9). However, validation of the scaling laws $t_h \sim h^{2/3}$ and $\phi_h \sim h^{-2/3}$ require additional experiments.

We end this section by providing a broader perspective on the paper cutting process and a statistical interpretation of the phase diagram (Fig. 3): paper cuts are associated with a range of activities across home, school, office, and industry environments. Although certain angles (ϕ) between finger and paper may be connected to particular activities, it is difficult to argue for the strong prevalence of any specific angle(s). Inspired by statistical mechanics, we consider the slicing angle ϕ as a random variable with a uniform probability distribution and examine the cutting probability $p(t)$ at a fixed paper thickness t across a range of angles $0 < \phi < \pi/2$. The likelihood of cutting during handling of the paper can then be described as the probability of paper handling at an angle below $\phi_c(t)$:

$$p(t) = \frac{\phi_c(t)}{\pi/2}. \tag{7}$$

Equation (7) provides a potential explanation for the erratic nature of paper cuts. As seen in Fig. 3, cutting mostly occurs for angles $\phi \leqslant 15^\circ$. However, at or near the most hazardous paper thickness t_h [Eq. (5)], there is a much greater chance of injury, $p(t_h) = \frac{\phi_c(t_h)}{\pi/2}$. Expressed in all system parameters, the change of injury at the most hazardous thickness is

$$p(t_h) = \frac{1}{\pi/2}\frac{\kappa\alpha^2}{(1-\nu^2)^{2/3}}\frac{\left(E_p^{1/2}E_s\right)^{2/3}}{\sigma_{t,c}}\left(\frac{d}{h}\right)^{2/3} \approx 21\,\%. \tag{8}$$

When handling the most hazardous paper, the chance of injury is thus roughly 1 in 5 averaged over many random interactions.

IV. DISCUSSION AND CONCLUSIONS

A fairly comprehensive picture of the physical processes that may reduce (or enhance) the dangers of paper cuts has emerged. First and foremost, we provide a rationale for the surprising observation that slicing only occurs when the paper edge is fine, but not too thin. The reason is that cutting into soft tissues requires a certain critical force. However, if the paper is overly fine, it buckles under the load before cutting can occur.

These results allow us to assess the relative safety of various product categories broadly. While tissues, books, and photos are generally safe, we cannot rule out certain risks of using office paper or magazines. In the future, paper manufacturers, printers, and publishing companies may wish to consider this during the product design process.

It is worth pointing out, however, that the habits and dexterity of the user also play a role. In particular, most paper cuts can be avoided by adhering to a strict near-normal-contact regimen (i.e., $\phi \rangle \phi_h \approx 20^\circ$), which minimizes the cutting likelihood. Regardless, we stress that more work is needed to assess the influence of the azimuthal slicing angle, and the relative safety of composite paper products, such as corrugated cardboard.

Identifying the most hazardous paper thickness may also allow for novel applications in cases where cutting is desirable. Indeed, we speculate that paper blades may offer a substitute for conventional metallic knives in cases such as

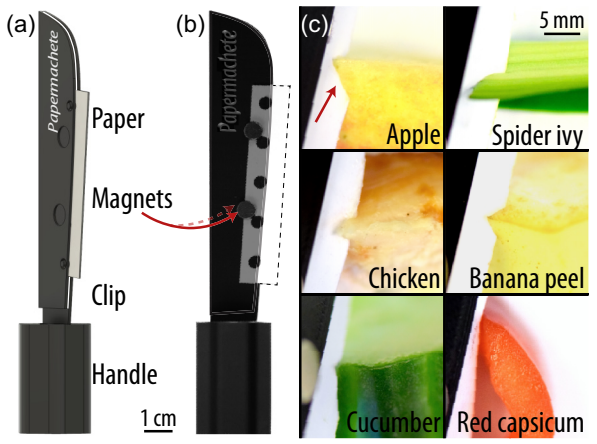

FIG. 4. The Papermachete uses discarded traction sections of dot-matrix paper as a blade. (a) Technical drawing and (b) photograph of the recyclable paper-knife. The single-use paper blade is fixed in the clip by magnets while the handle facilitates convenient use. (c) The Papermachete can cut into a variety of plant- and animal-based products. The cuts were performed by hand at the slicing angle of $\phi \approx 10^\circ$ at speeds of approximately 1 cm/s in the direction of the arrow.

cooking and dining [28], and, perhaps, in the textile industry and home gardening. The regular occurrence of paper cuts also demonstrates that paper may have a future role in transdermal drug delivery [29] if, for instance, the drug is mixed into the paper matrix. Stimulated by these ideas, we designed and 3D printer, the *Papermachete* [Figs. 4(a) and 4(b)], which utilizes discarded traction sections of dot-matrix paper as a blade. (See the Supplemental Material for design files [14].) The Papermachete easily cuts into most soft plant- and animal-based products [Fig. 4(c)]; however, it is not suitable, for example, for wood carving and spreading butter. Despite its seemingly mundane nature, studying the physics of paper cuts has revealed a surprising potential use for paper in the digital age: not as a means of information dissemination and storage but rather as a tool of destruction.

APPENDIX A: SURFACE CHARACTERIZATION

Experiments are performed to elucidate the link between paper thickness and the occurrence of paper cuts. An attempt to slice into a gelatin block with a sheet of paper is made. The interaction is recorded, and tangential and normal stresses are measured. Each attempt is categorized. First, we introduce the three rough categories: buckling of the paper, cutting, and

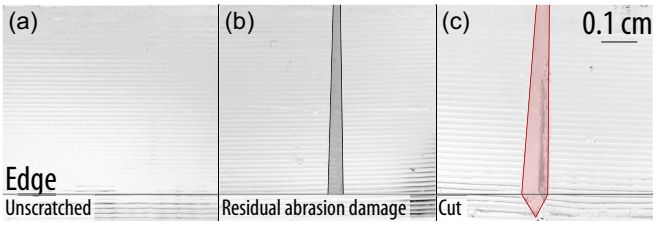

FIG. 5. Definitions of surface characteristics after the experiment. The horizontal line is the edge and is included to demonstrate the cut into the sample.

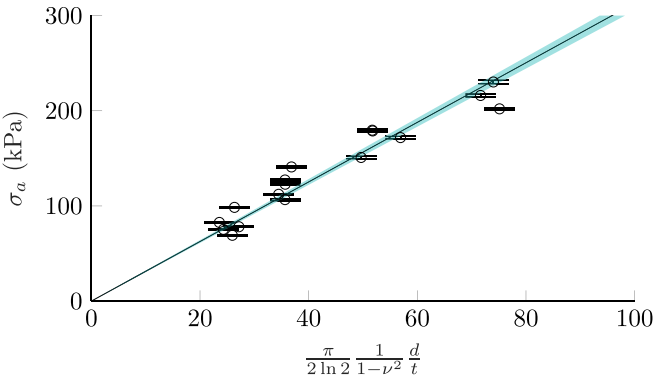

FIG. 6. Measured maximum applied stress σ_a plotted as a function of relative indentation depth d/t (dots). An unweighted least-squares to Eq. (2) yields the estimate $E_s = 3.13 \pm 0.08$ kPa (solid line).

indentation into the soft gelatin. Both video (see the Supplemental Material [14]) and visual inspection of the substrate surface (Fig. 5) after the experiment are used to determine the cutting dynamics. While the contact between the paper sheet and gelatin might leave residual abrasions even though buckling or indentation is observed, they are distinguishable from the slashed surface appearing after a cut.

APPENDIX B: YOUNG'S MODULUS OF GELATIN

The outcome of the interaction between a sheet of paper and a substrate depends in part on the softness of the substrate. Young's modulus of the gelatin, E_s, is measured using a normal-indentation-test using a rectangular indenter attached to a vertical stage. The indenter (a sheet of paper) traveled $d \approx 2$ mm into the gelatin slab. Experiments are performed with indenters of thickness $t = 0.076{-}0.245$ mm, and no buckling was observed. E_s is determined by fitting data to

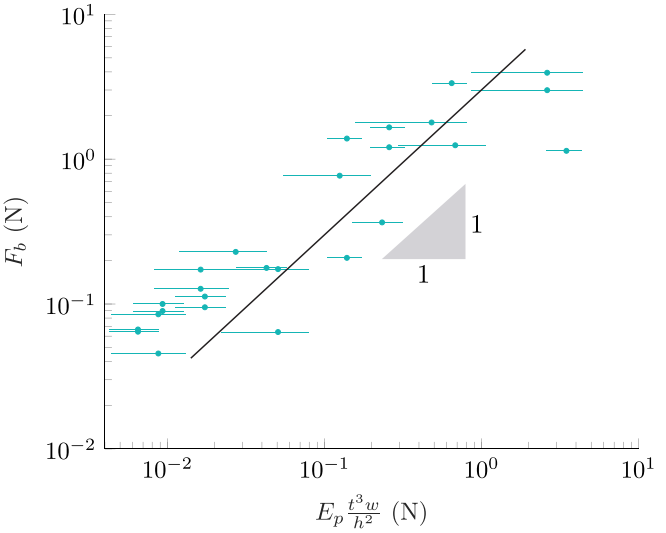

FIG. 7. Experimentally measured buckling force compared to Euler's beam equation, which stipulates $F_b \sim E_p t^3 w/h^2$. Here, E_p is the paper's elastic modulus, t and w its thickness and width, and h the free height of the sheet (Fig. 1 in the text). Data compare reasonably well with the simple model.

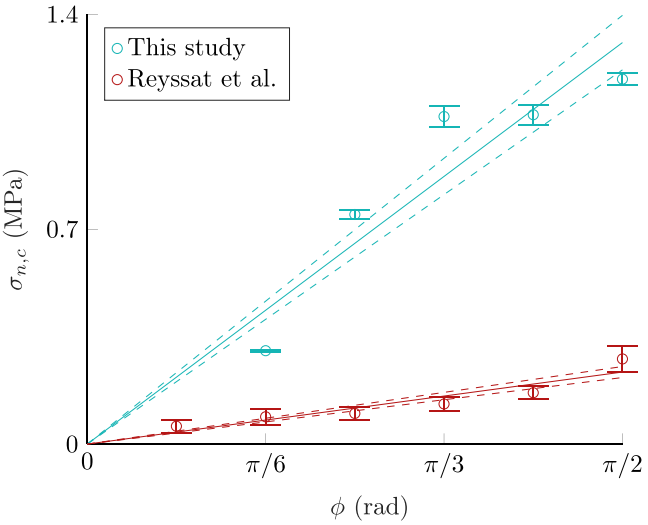

FIG. 8. The normal stress $\sigma_{n,c}$ required for the onset of cutting diminishes with slicing angle ϕ. Our experimental data (blue) as well as data from Reyssat *et al.* [11] are not inconsistent with a linear fit according to Eq. (7): (solid line) derived from the numerical model proposed [11]. The fitted slope is the material parameter $\sigma_{t,c} = 0.84 \pm 0.06$ MPa.

a contact mechanics model describing the relation between stress and strain (indentation depth) for a rigid rectangular punch in contact with an elastic half-space [Eq. (2)] [16]. An unweighted least-squares linear fit with no intercept between measured applied stress, σ_a, and the normalized strain, $\pi d/[2\ln 2(1-\nu^2)t]$, is performed [30] (Fig. 6). The fitted slope is $E_s = 3.13 \pm 0.08$ kPa. Data compares reasonably well with the linear model (Fig. 6).

This modulus is relatively small compared to values obtained by, for example, Taberlet *et al.* [31] and Forte *et al.* [32], who observed $E_s \approx 10 - 80$ kPa. However, it has been demonstrated that the elastic modulus is affected by temperature [33] and aging [34] (see also Ref. [31]). We therefore speculate that the difference is due to the specific production and setting conditions used in the present study.

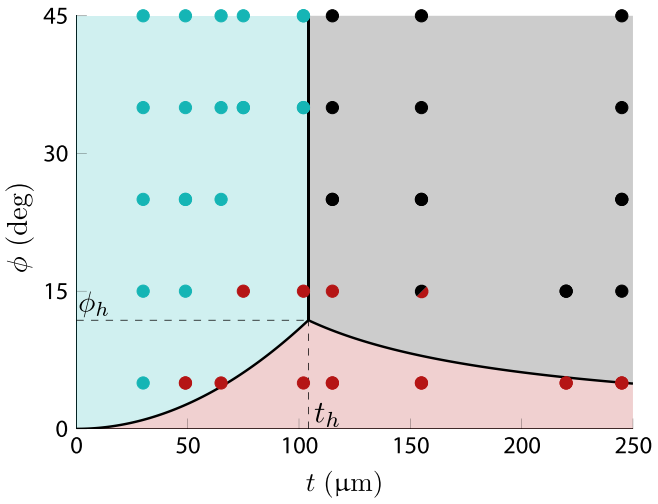

FIG. 9. Phase diagram constructed for paper height $h = 28$ mm (i.e., twice the height used to construct the phase diagram in Fig. 3). Peaks at the most hazardous thickness $t_h \approx 105\,\mu$m m (between printed magazines and office paper) and angle $\phi_h \approx 12^\circ$.

APPENDIX C: VALIDITY OF EULER'S BUCKLING EQUATION

Complex dynamics arise when the sheet buckles against the gelatin. To rationalize the experimental data, we employ the simple Euler's beam theory [Eq. (3)]. To determine the validity of this result, we measure the buckling force and compare it to the model, which stipulates $F_b \sim E_p t^3 w/h^2$. Here, E_p is the paper's elastic modulus, t and w its thickness and width, and h the free height of the sheet (Fig. 1). Data (Fig. 7) compare reasonably well with the simple model. Based on this result, we propose that effects such as complex forces due to a limited contact line and flexural instabilities can be neglected.

APPENDIX D: CRITICAL CUTTING STRESS

The critical cutting stress threshold must be exceeded for cutting to occur. At cutting onset, the critical stresses are respectively denoted $\sigma_{n,c}$ and $\sigma_{t,c}$, where $\sigma_{n,c} = \sigma_{t,c}\tan\phi$. For small angles, this is approximately $\sigma_{n,c} \approx \sigma_{t,c}\phi$. To investigate whether the small angle approximation is valid, we measure $\sigma_{n,c}$ for angles in the range $\phi = 30^\circ - 90^\circ$. These results are plotted alongside data obtained by Reyssat *et al.* [11] (Fig. 8). While the small angle approximation is not inconsistent with experimental data beyond its classical validity, our cutting attempt only yields cutting up to $\phi = 20^\circ$, where the deviation from the full expression is ≈4%. For the experimentally relevant angles, the linear model should sufficiently predict the cutting thresholds.

APPENDIX E: PHASE DIAGRAM FOR $h = 28$ mm

Our stress analysis indicates that the free paper height h influences the cutting process [Eqs. (5) and (6)]. To quantify how the domains shift, we obtain experimental data where the paper height is doubled from $h = 14$ mm to $h = 28$ mm. The resulting phase diagram shows that increasing h increases the most hazardous thickness and shifts the corresponding angle ϕ_h downward (Fig. 9).

TABLE I. Paper samples used in our experiments. The error is ±5 μm for the thickness measurements.

Product	Brand	Area density g/m^2	t μm	E_p MPa
Tissue	Creativ Co.	12.7 ± 1.8	30	0.4 ± 0.3
Printed magazine	Nature	48.8 ± 0.2	49	7.1 ± 1.2
Printed magazine	Science	56.9 ± 1.2	55	7.2 ± 1.6
Newspaper	Information	41.6 ± 0.7	65	8.1 ± 1.8
Dot matrix	Top List	56.6 ± 0.6	65	4.1 ± 1.8
Post its	Stick'n	60.5 ± 0.3	75	9.2 ± 0.2
Office paper	Multicopy	79.6 ± 0.5	102	3.3 ± 1.8
Card stock	Panduro	89 ± 2	115	2.7 ± 0.3
Office paper	ColorChoice	158.3 ± 1.5	155	4.8 ± 1.1
Metallic paper	Panduro	123.9 ± 1.0	165	3 ± 2
Photo paper	Bog & Ide	184 ± 3	220	1.7 ± 0.4
Office paper	Xerox	241.9 ± 1.8	245	3.2 ± 0.8

[1] L. Peterson, L. Saldana, and N. Heiblum, Quantifying tissue damage from childhood injury: The minor injury severity scale, J. Pediatr. Psychol. **21**, 251 (1996).

[2] M. Roser and E. Ortiz-Ospina, Literacy, our world in data (2016), https://ourworldindata.org/literacy.

[3] S. L. DeBoer and D. Zeglin, Necrotizing fasciitis: Even with optimal treatment, the mortality rate is 40%, Am. J. Nurs. **101**, 37 (2001).

[4] A. H. Milby, N. D. Pappas, J. O'Donnell, and D. J. Bozentka, Sporotrichosis of the upper extremity, Orthopedics **33**, 273 (2010).

[5] S. Mirsky, The unkindest cut, Sci. Am. **306**, 80 (2012).

[6] J. C. McKeown, *A Cabinet of Ancient Medical Curiosities: Strange Tales and Surprising Facts from the Healing Arts of Greece and Rome* (Oxford University Press, Oxford, 2016).

[7] D. Zhou and G. McMurray, Modeling of blade sharpness and compression cut of biomaterials, Robotica **28**, 311 (2010).

[8] S. Mora and Y. Pomeau, Cutting and slicing of weak solids, Phys. Rev. Lett. **125**, 038002 (2020).

[9] A. G. Atkins, X. Xu, and G. Jeronimidis, Cutting, by 'pressing and slicing,' of thin floppy slices of materials illustrated by experiments on cheddar cheese and salami, J. Mater. Sci. **39**, 2761 (2004).

[10] A. Spagnoli, R. Brighenti, M. Terzano, and F. Artoni, Cutting resistance of soft materials: Effects of blade inclination and friction, Theor. Appl. Fract. Mech. **101**, 200 (2019).

[11] E. Reyssat, T. Tallinen, M. Le Merrer, and L. Mahadevan, Slicing softly with shear, Phys. Rev. Lett. **109**, 244301 (2012).

[12] Y. Liu, C.-Y. Hui, and W. Hong, A clean cut, Extreme Mech. Lett. **46**, 101343 (2021).

[13] A. Atkins, Slice–push, formation of grooves and the scale effect in cutting, Interface Focus **6**, 20160019 (2016).

[14] See Supplemental Material at http://link.aps.org/supplemental/10.1103/PhysRevE.110.025003 for design files of experimental setup and *Papermachete* and video of cutting experiments.

[15] P. W. Johnson and J. M. Blackstone, Children and gender-differences in exposure and how anthropometric differences can be incorporated into the design of computer input devices, Scand. J. Work Environ. Health **33**, 26 (2007).

[16] P. Brothers, G. Sinclair, and C. Segedin, Uniform indentation of the elastic half-space by a rigid rectangular punch, Int. J. Solids Struct. **13**, 1059 (1977).

[17] M. Oldfield, D. Dini, T. Jaiswal, and F. Rodriguez y Baena, The significance of rate dependency in blade insertions into a gelatin soft tissue phantom, Tribol. Int. **63**, 226 (2013).

[18] S. Komandur, P. W. Johnson, R. L. Storch, and M. G. Yost, Relation between index finger width and hand width anthropometric measures, in *2009 Annual International Conference of the IEEE Engineering in Medicine and Biology Society* (IEEE, Minneapolis, MN, USA, 2009), pp. 823–826.

[19] B. Lautrup, *Physics of Continuous Matter: Exotic and Everyday Phenomena in the Macroscopic World* (CRC Press, Boca Raton, FL, 2011).

[20] S. Fakhouri, S. B. Hutchens, and A. J. Crosby, Puncture mechanics of soft solids, Soft Matter **11**, 4723 (2015).

[21] S. P. Timoshenko and J. M. Gere, *Theory of Elastic Stability* (Courier Corporation, North Chelmsford, MA, 2009).

[22] T. Barois, I. Jalisse, L. Tadrist, and E. Virot, Transition to stress focusing for locally curved sheets, Phys. Rev. E **104**, 014801 (2021).

[23] M. Czerner, L. A. Fasce, J. F. Martucci, R. Ruseckaite, and P. M. Frontini, Deformation and fracture behavior of physical gelatin gel systems, Food Hydrocoll. **60**, 299 (2016).

[24] O. A. Shergold and N. A. Fleck, Experimental investigation into the deep penetration of soft solids by sharp and blunt punches, with application to the piercing of skin, J. Biomed. Eng. **127**, 838 (2005).

[25] M. Terzano, A. Spagnoli, and P. Ståhle, A fracture mechanics model to study indentation cutting, Fatigue Fract. Eng. Mater. Struct. **41**, 821 (2018).

[26] A. Spagnoli, M. Terzano, R. Brighenti, F. Artoni, and P. Ståhle, The fracture mechanics in cutting: A comparative study on hard and soft polymeric materials, Int. J. Mech. Sci. **148**, 554 (2018).

[27] V. Normand, S. Muller, J.-C. Ravey, and A. Parker, Gelation kinetics of gelatin: A master curve and network modeling, Macromolecules **33**, 1063 (2000).

[28] H. N. Patil and P. Sinhal, A study on edible cutlery: An alternative for conventional ones, Atithya **4**, 45 (2018).

[29] M. R. Prausnitz and R. Langer, Transdermal drug delivery, Nat. Biotechnol. **26**, 1261 (2008).

[30] R. Taylor John, *An Introduction to Error Analysis* (University Science Books, Sausalito, CA, 1997).

[31] N. Taberlet, J. Ferrand, É. Camus, L. Lachaud, and N. Plihon, How tall can gelatin towers be? An introduction to elasticity and buckling, Am. J. Phys. **85**, 908 (2017).

[32] A. Forte, F. D'amico, M. Charalambides, D. Dini, and J. Williams, Modelling and experimental characterisation of the rate dependent fracture properties of gelatine gels, Food Hydrocoll. **46**, 180 (2015).

[33] A. D. Doyle and J. Lee, Simultaneous, real-time imaging of intracellular calcium and cellular traction force production, BioTechniques **33**, 358 (2002).

[34] A. Bot, I. A. van Amerongen, R. D. Groot, N. L. Hoekstra, and W. G. Agterof, Large deformation rheology of gelatin gels, Polym. Gels Networks **4**, 189 (1996).